

## Structural, Thermal and Electrical Properties of $\text{Li}_{4-2x}\text{Zn}_x\text{SiO}_4$ Ceramic Electrolyte Prepared by Citrate Sol Gel Technique

S.B.R.S Adnan<sup>1,\*</sup> and N.S. Mohamed<sup>2</sup>

<sup>1</sup>Institute of Graduate Studies, University of Malaya, 50603 Kuala Lumpur, Malaysia

<sup>2</sup>Centre for Foundation Studies in Science, University of Malaya, 50603 Kuala Lumpur, Malaysia

\*E-mail: [syed\\_bahari@yahoo.com](mailto:syed_bahari@yahoo.com); [nsabirin@um.edu.my](mailto:nsabirin@um.edu.my)

Received: 17 November 2012 / Accepted: 5 April 2013 / Published: 1 May 2013

---

The aim of this work is to investigate the structural, thermal and electrical properties of Zn doped  $\text{Li}_4\text{SiO}_4$  synthesized by a sol gel method. The formation of the compound is confirmed by X-ray diffraction study. Thermal properties of the compounds are measured using DSC analysis while the electrical characteristics are investigated by impedance spectroscopy. The introduction of zinc ions considerably raises the conductivity and improves thermal stability of the parent compound  $\text{Li}_4\text{SiO}_4$ . The compound of  $\text{Li}_{3.88}\text{Zn}_{0.06}\text{SiO}_4$  gives a maximum value of  $3.2 \times 10^{-5} \text{ S cm}^{-1}$  at room temperature and  $1.08 \times 10^{-3} \text{ S cm}^{-1}$  at 500 °C. The charge carrier concentration, mobile ion concentration and ion hopping rate are calculated by fitting the conductance spectra to power law variation,  $\sigma_{ac}(\omega) = \sigma_o + A\omega^a$ . The charge carrier concentration and mobile ion concentration are found to be constant over the temperature range from 303 K to 773 K while mobility of ion increases with temperature implying that the increase in conductivity with temperature is due to increase in ion mobility. The transference number corresponding to  $\text{Li}^+$  ion transport determined by means of Bruce and Vincent technique shows that majority charge carriers in the compound are  $\text{Li}^+$  ions.

---

**Keywords:** Arrhenius, ceramic, electrolyte,  $\text{Li}_4\text{SiO}_4$ , sol gel, transference number

### 1. INTRODUCTION

Interest in ceramic solid-state electrolytes has led to a widespread search for ionically conducting materials. However, the solid-state electrolytes composition must be tuned to readily admit ions, while simultaneously forming safe, impenetrable and electronically insulating barriers [1]. The role of the electrolyte is to provide an ionic conduction path between anode and the cathode in electrochemical devices such as fuel cell, super capacitors, secondary batteries etc. As such, the prime

concern in electrolyte research is to enhance ionic conductivity which is the main challenge faced by researchers in this field.

In the search for a variety of batteries and solid state electrolyte with  $\text{Li}^+$  ion conductors, considerable interest has been shown in systems based on lithium orthosilicate ( $\text{Li}_4\text{SiO}_4$ ) which is chemically stable [2-16].  $\text{Li}_4\text{SiO}_4$  exist in two polymorphic forms which are separated by a broad transition region between 600 °C and 725 °C [2]. The crystal structure of this compound consists of lithium-oxygen polyhedral which represent the lithium sites, are connected together by multiple sharing of faces to form three dimension network of cages linked by triangular windows. On average, the lithium sites are less than half full and so there are also plenty of other sites which are unoccupied but could be occupied transiently and afford extra conduction pathways [2,5,10].

$\text{Li}_4\text{SiO}_4$ , itself is a poor conductor ( $\sigma_{RT} = 10^{-8}$ - $10^{-6}$  S  $\text{cm}^{-1}$ ) [2,5,17]. However, its conductivity can be greatly enhanced by aliovalent doping such as  $\text{Li}_{4-2x}\text{D}_x\text{SiO}_4$  ( $D = \text{Co}^{2+}$ ,  $\text{Ni}^{2+}$ ,  $\text{Mg}^{2+}$ )[5,8],  $\text{Li}_{4-3x}\text{T}_x\text{SiO}_4$  ( $T = \text{Al}^{3+}$ ,  $\text{Ga}^{3+}$ ,  $\text{B}^{3+}$ ,  $\text{In}^{3+}$ )[4,6-9,15-16] and  $\text{Li}_{4-x}\text{M}_x\text{Si}_{1-x}\text{O}_4$  ( $M = \text{V}^{5+}$ ,  $\text{As}^{5+}$ ,  $\text{P}^{5+}$ ) [11-14]. These doping may create vacant sites in the crystal and any lithium ion in the immediate vicinity can jump to the vacant sites. This leaves the previous site of the ion vacant which could now host another ion. This results the transport of ions across the solid giving rise to conductivity. Their concentration is the main factor determining the conductivity of this solid electrolyte [18].

West [10] has reported previously the conductivity data for the  $\text{Li}_{3.4}\text{Zn}_{0.3}\text{SiO}_4$  compound at temperature 450 °C to 700 °C with conductivity value  $3.4 \times 10^{-4}$  S  $\text{cm}^{-1}$  and  $2.3 \times 10^{-2}$  S  $\text{cm}^{-1}$  respectively using conventional solid state reaction. However, the works reported in the literature only focused for high temperature application (>450 °C). No works on this type material for low and medium temperature devices application has been reported. Such study is interesting one as development of the electrolytes with high conductivity at low and medium temperatures can broaden their use to low and medium temperature solid state devices such as in energy and transportation sector, communication electronics, display devices, medicine and metallurgy.

Meanwhile, the synthesis using citrate sol gel technique has been reported can enhance the conductivity compared to the conventional solid state reaction [19]. Furthermore, this technique has other advantages such as lowering the synthesis temperature, effective in improving the linkage between grain boundary, molecular-level homogeneity can be easily achieved and the homogeneous mixture containing all the compounds in the correct stoichiometry ensures a much higher purity of the sample. This method is also simple and therefore suitable for both small scale and large scale production. [2-3,19-20].

In the author's previous work,  $\text{Li}_4\text{SiO}_4$  compound has been successfully prepared using this method. The compound exhibited conductivity of  $1.16 \times 10^{-4}$  S  $\text{cm}^{-1}$  at 100°C [2]. This conductivity is an order of magnitude higher compared to the value of compound prepared by solid state reaction method reported by Smith and West, 1990 [21]. In this work,  $\text{Li}_{4-2x}\text{Zn}_x\text{SiO}_4$  ( $x = 0, 0.06, 0.12, 0.20$ ) compound were prepared by the same sol gel method. The structural, thermal and electrical properties using x-ray diffraction (XRD), differential scanning calorimetry (DSC) and impedance spectroscopy were studied.

## 2. EXPERIMENTAL PROCEDURE

### 2.1 Synthesis of $Li_{4-2x}Zn_xSiO_4$

In this study, four compounds with  $x = 0, 0.06, 0.12, 0.20$  were prepared via sol gel technique. For sample preparation, lithium acetate ( $C_2H_3LiO_2$ ) zinc acetate ( $C_4H_{10}O_6Zn$ ) and tetraethyl orthosilicate ( $SiC_8H_{20}O_4$ ) were used as the starting materials. Meanwhile citric acid was used as the chelating agent. Lithium acetate and zinc acetate were dissolved in distilled water and later mixed with citric acid under magnetic stirring. The solution was transferred into a reflux system and continuously stirred until a homogeneous solution was formed. Solution of tetraethyl orthosilicate was then added to the homogeneous solution. After stirring for 12 hours, the solution was taken out and then vaporized for about two hours under magnetic stirring at  $75\text{ }^\circ\text{C}$ . The resulting wet gel was dried in an oven at  $150\text{ }^\circ\text{C}$  for 24 hours to remove water particles, resistance organic groups as well as to avoid ceramic cracks. The powder was pressed using a Specac pellet hydraulic press to form pellet with diameter and thickness of 13 mm and 2 mm respectively. The pellets were later sintered at  $850\text{ }^\circ\text{C}$  for 12 hours.

### 2.2. Characterization techniques.

Bruker AXS D8 X-ray diffractometer employing  $Cu-K_\alpha$  radiation was used to perform X-ray diffraction in order to identify the crystalline phase of the material. Thermal behavior of the sintered sample was analyzed by differential scanning calorimetry (DSC) (EVO Lab<sup>sys</sup> thermal analyzer) in  $N_2$  atmosphere at a constant heating rate of  $10\text{ }^\circ\text{C}/\text{min}$  in the temperature range between room temperature and  $1300\text{ }^\circ\text{C}$ . The compounds electrical properties were determined by ac impedance spectroscopy using Solatron 1260 impedance analyzer over a frequency range from 0.1 to  $10^6$  Hz. An applied voltage was fixed at 110 mV.

The dc conductivity was determined using the equation:

$$\sigma_b = \frac{d}{AR_b} \quad (1)$$

where  $d$  is the sample thickness,  $A$  is the area of the electrode and  $R_b$  is the bulk resistance which is determined from impedance plot.

The ac conductivity has been evaluated from dielectric data in accordance with the relation:

$$\sigma_{ac} = \omega \epsilon_0 \epsilon'' \tan \delta \quad (2)$$

where  $\epsilon_0$  is permittivity of the free space ( $8.854 \times 10^{-14} \text{ F cm}^{-1}$ ),  $\omega$  is  $2\pi f$ ,  $\epsilon''$  is dielectric loss and  $\tan \delta$  is the dielectric loss factor. Lithium transference number measurement was done using Bruce and Vincent method [22-24] in order to determine the actual type of charge carriers. This method requires characterization of cell before and after polarization (after reaching the steady state) by using combination of EIS and DC polarization technique. For this measurement the samples were

sandwiched between lithium metal electrodes which are used as non-blocking electrodes that only allow  $\text{Li}^+$  ions to transfer. The lithium transference number ( $\tau_{\text{Li}^+}$ ) was calculated using the equation:

$$\tau_{\text{Li}^+} = \frac{I_{ss}(\Delta V - I_o R_o)}{I_o(\Delta V - I_{ss} R_{ss})} = \frac{R_e}{\left(\frac{\Delta V}{I_{ss}} - R_{ss}\right)} \quad (3)$$

In this equation,  $I_o$  is initial current ( $t = 0$ ),  $I_{ss}$  is steady state current,  $R_o$  and  $R_{ss}$  are initial resistance of the passive layer (before polarization) and resistance of the passive layer (after polarization) respectively and  $\Delta V$  is applied voltage bias ( $\Delta V = 500$  mV).  $R_e$  is resistance of the electrolyte which is calculated using Ohm's law:

$$R_e = \frac{\Delta V}{I_o} - R_o \quad (4)$$

### 3. RESULT AND DISCUSSION

#### 3.1. Structural properties

Fig. 1(a) presents the XRD spectra of all the  $\text{Li}_{4-2x}\text{Zn}_x\text{SiO}_4$  samples. The XRD spectra of all samples can be indexed to monoclinic structure in space group  $P2_1/m$  [25].

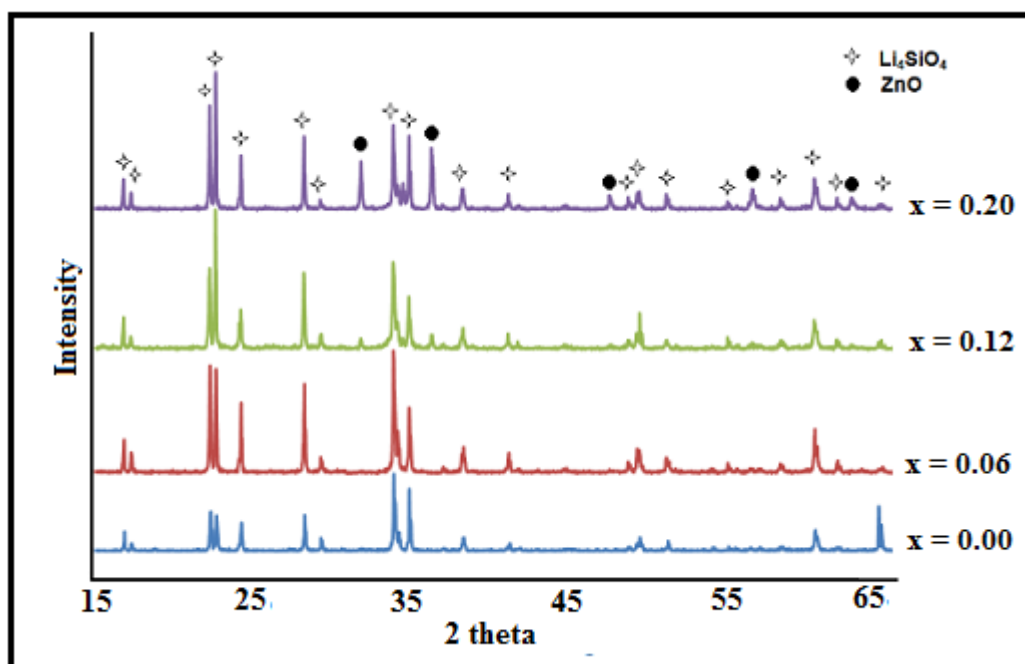


**Figure 1.** XRD pattern of  $\text{Li}_{4-2x}\text{Zn}_x\text{SiO}_4$  samples

**Table 1.** Lattice parameters of the  $Li_{4-2x}Zn_xSiO_4$  samples

Samples	$a$ (Å)	$b$ (Å)	$c$ (Å)	$\beta$ (°)	$V$ (Å <sup>3</sup> )
$x = 0.00$	5.147	6.094	5.293	90.33	166.01
$x = 0.06$	5.295	6.098	5.149	90.32	166.20
$x = 0.12$	5.296	6.099	5.147	90.31	166.25
$x = 0.20$	5.297	6.102	5.150	90.25	166.46

Compared with the XRD spectra of the  $Li_4SiO_4$  sample, single phase solid electrolyte only appear in the sample with  $x=0.06$  which shows no extra peaks in its XRD spectrum. The peaks shift to higher diffraction angle indicating that  $Zn^{2+}$  ion is in the  $Li_4SiO_4$  structure rather than forming impurities. The diffraction peaks are also broadened by Zn doping, which implies that the crystal size decreases with increasing Zn content. The peak at diffraction angle  $65^\circ$  tends to disappear with increasing Zn amount. Meanwhile, small peaks attributed to ZnO arise in XRD patterns appear in the sample doped with  $x=0.12$  and  $x=0.20$ .

The lattice parameters of the  $Li_{4-2x}Zn_xSiO_4$  samples are listed in Table 1. The parameters of  $Li_4SiO_4$  are in good agreement with the values reported by Dubey and West [26]. The value of  $a$ ,  $b$  and  $V$  (unit cell volume) increase with increasing  $x$  and the value of  $c$  is first decreases and then increases with increasing  $x$ . Among all of the lattice parameters, monoclinic angle  $\beta$  decreases slightly with increasing  $x$ . The increase in the unit cell volume is mostly related to the  $Zn^{2+}$  insertion into  $Li_4SiO_4$  structure which can be attributed to the larger atomic size of  $Zn^{2+}$  (0.74 Å) than that of  $Li^+$  (0.68 Å) [7,27].

### 3.2. Thermal properties

The DSC curves for  $Li_{4-2x}Zn_xSiO_4$  samples are shown in Fig. 2. There are three endothermic peaks in the curve of the sample with  $x = 0$ . The first peak is located in temperature range from  $60^\circ C$  to  $120^\circ C$  due to evaporation of water process. The intensity of the peak decreases with the increase of  $x$  and disappears in the sample with  $x = 0.12$  and  $0.20$ . The second peak which is observed in temperature range from  $550^\circ C$  to  $610^\circ C$  is recognized as second order phase transition of  $Li_4SiO_4$ . A similar observation has been reported by other researchers [10,28-30]. The third peak which has maximum peak at temperature of  $1027^\circ C$  represents the melting temperature of the sample. Increasing  $x$  value results in an increase in phase transition and melting temperature which is in contrast to the result of West [10] who reported the substitution of zinc in  $Li_4SiO_4$  lowers the temperature of phase transition. The increases in  $x$  as well as increase in phase transition and melting temperature indicate enhancement in thermal stability of the ceramic upon substitution of  $Zn^{2+}$  ions for  $Li^+$  ions. The broad endothermic peak observed in the DSC curve of the samples with  $x = 0.12$  and  $x = 0.20$  at temperature range  $600^\circ C$  -  $1000^\circ C$  may be due to the presence of ZnO impurities in the samples.

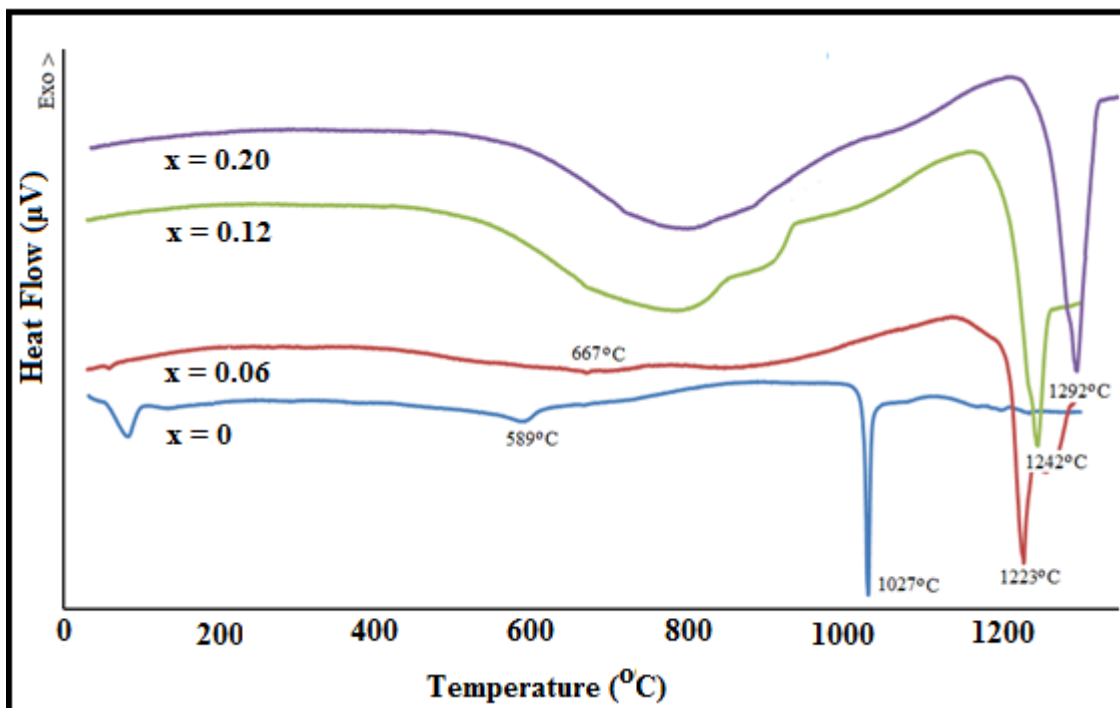


**Figure 2.** DSC curves of  $Li_{4-2x}Zn_xSiO_4$  samples.

### 3.3. Electrical properties

#### 3.3.1 Dc conductivity

The dc conductivity of  $Li_{4-2x}Zn_xSiO_4$  was determined from the bulk resistance,  $R_b$  using equation (1). The dc conductivity for all samples at 500 °C and RT are listed in Table 2. The maximum conductivity is observed at  $x = 0.06$  with conductivity value of  $3.20 \times 10^{-5} \text{ S cm}^{-1}$  at RT and increases to  $1.08 \times 10^{-3} \text{ S cm}^{-1}$  at 500°C. The conductivity increases by an order of magnitude compared to the  $Li_4SiO_4$  with replacement of  $Li^+$  to  $Zn^{2+}$ . Even though the solubility of zinc in this electrolyte is low, small addition of  $Zn^{2+}$  significantly raises the conductivity. The conductivity decreases with further increase in  $x$  due to the presence of the impurities, ZnO which may block the migration of  $Li^+$  ion between grains. However, the conductivity of the samples with  $x = 0.12$  and  $x = 0.20$  is still higher than that of  $Li_4SiO_4$ . This effect is due to the increase of cation vacancies in the monoclinic structure [5].

**Table 2.** Conductivity data for  $Li_{4-2x}Zn_xSiO_4$  samples at ambient temperature and 500 °C

Samples	$\sigma_{500} (\text{S cm}^{-1})$	$\sigma_{RT} (\text{S cm}^{-1})$
$x = 0.00$	$1.00 \times 10^{-4}$	$9.36 \times 10^{-6}$
$x = 0.06$	$1.08 \times 10^{-3}$	$3.20 \times 10^{-5}$
$x = 0.12$	$3.00 \times 10^{-4}$	$2.60 \times 10^{-5}$
$x = 0.20$	$5.54 \times 10^{-4}$	$2.70 \times 10^{-5}$

The temperature dependence of the d.c conductivity of  $\text{Li}_{4-2x}\text{Zn}_x\text{SiO}_4$  samples is shown in Fig.3. The activation energy,  $E_a$  of the dc conductivity is calculated according to the Arrhenius equation:

$$\sigma_b T = A \exp \left( \frac{-E_a}{kT} \right) \tag{5}$$

where  $A$  is the pre-exponential factor,  $E_a$  is the activation energy for conduction and  $k$  is the Boltzman constant. The conductivity of all samples increases with temperature. However, all the  $\sigma$ - $1000/T$  plots show a discontinuity at  $\sim 300$  °C ( $1000/T = 1.75 \text{ K}^{-1}$ ) which is in agreement with the results reported by Wakihara et al [5] but in contrast to the result of West [10] who reported a discontinuity at 180 °C for  $\text{Li}_4\text{SiO}_4$ . The change in slope of  $\sigma$ - $1000/T$  plots could be due to an order-disorder transition of  $\text{Li}^+$  and  $\text{Zn}^{2+}$  ions since there is no experimental evidence for a phase transition occurring in the sample upon heating at room temperature until 500 °C as shown in Fig. 2. In the other words, the conductivity may be influenced at even slightest change in structure arrangement [5].

The activation energy for all samples which was extracted from the Arrhenius plots is shown in Fig. 4. The low value of activation energy indicates high mobility of ions in the sample. However, the presence of impurities in the samples of  $x = 0.12$  and  $x = 0.20$  lowers the ionic mobility and decreases the conductivity [31].

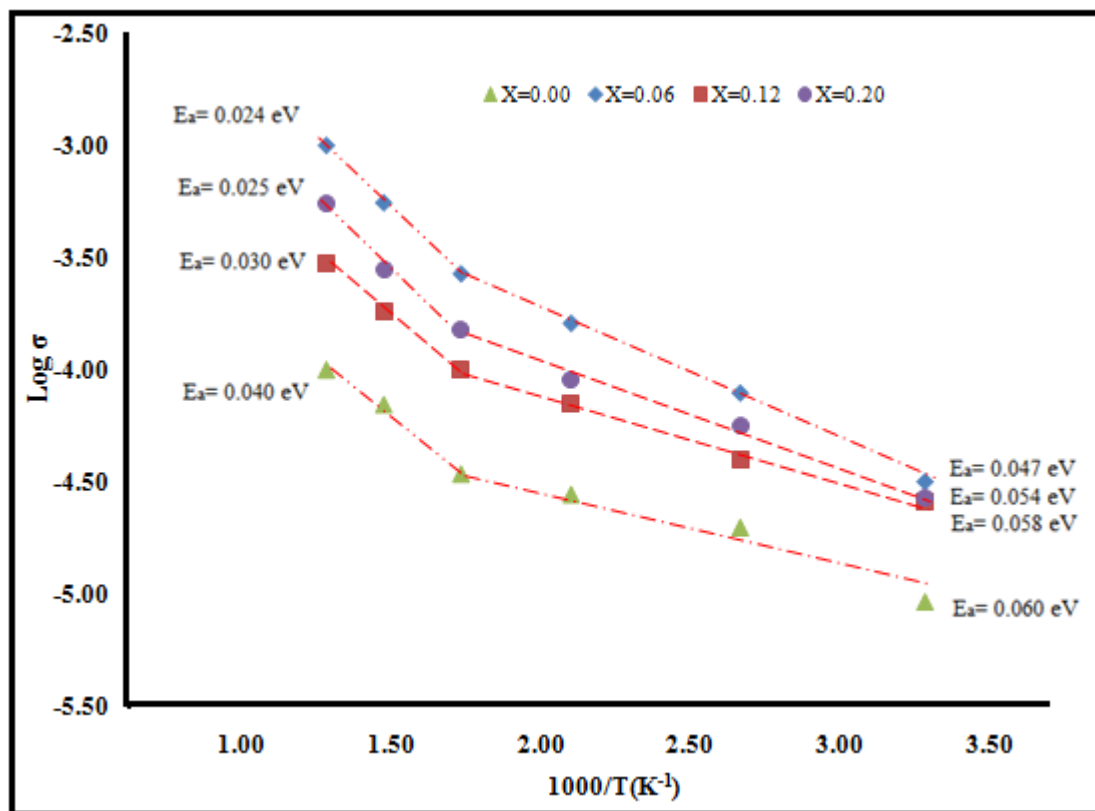


Figure 3. Arrhenius plot of the dc conductivity for sample  $\text{Li}_{4-2x}\text{Zn}_x\text{SiO}_4$  ( $x = 0, 0.06, 0.12, 0.20$ )

3.3.2 Conductivity spectra

Conductivity spectra for  $\text{Li}_{4-2x}\text{Zn}_x\text{SiO}_4$  samples at various temperatures are presented in Figure 4. At low frequencies, a plateau characterizes the dc conductivity. At high frequencies, conductivity increases according to universal power law. The conductivity can thus be represented by the expression as follows:

$$\sigma'(\omega) = \sigma(0) + A\omega^\alpha \tag{6}$$

where  $\sigma(0)$  is the d.c conductivity of the sample,  $A$  is a temperature dependant parameter and  $\alpha$  is the power law exponent which represents the degree of interaction between the mobile ion and is less than 1. When temperature increases, the transition from the d.c plateau to a.c conductivity dispersion region shifts towards higher frequency range. At high frequencies, the conductance spectra at different temperatures converge. This indicates that a.c conductivity is independent of temperature at high frequencies [2,32-36].

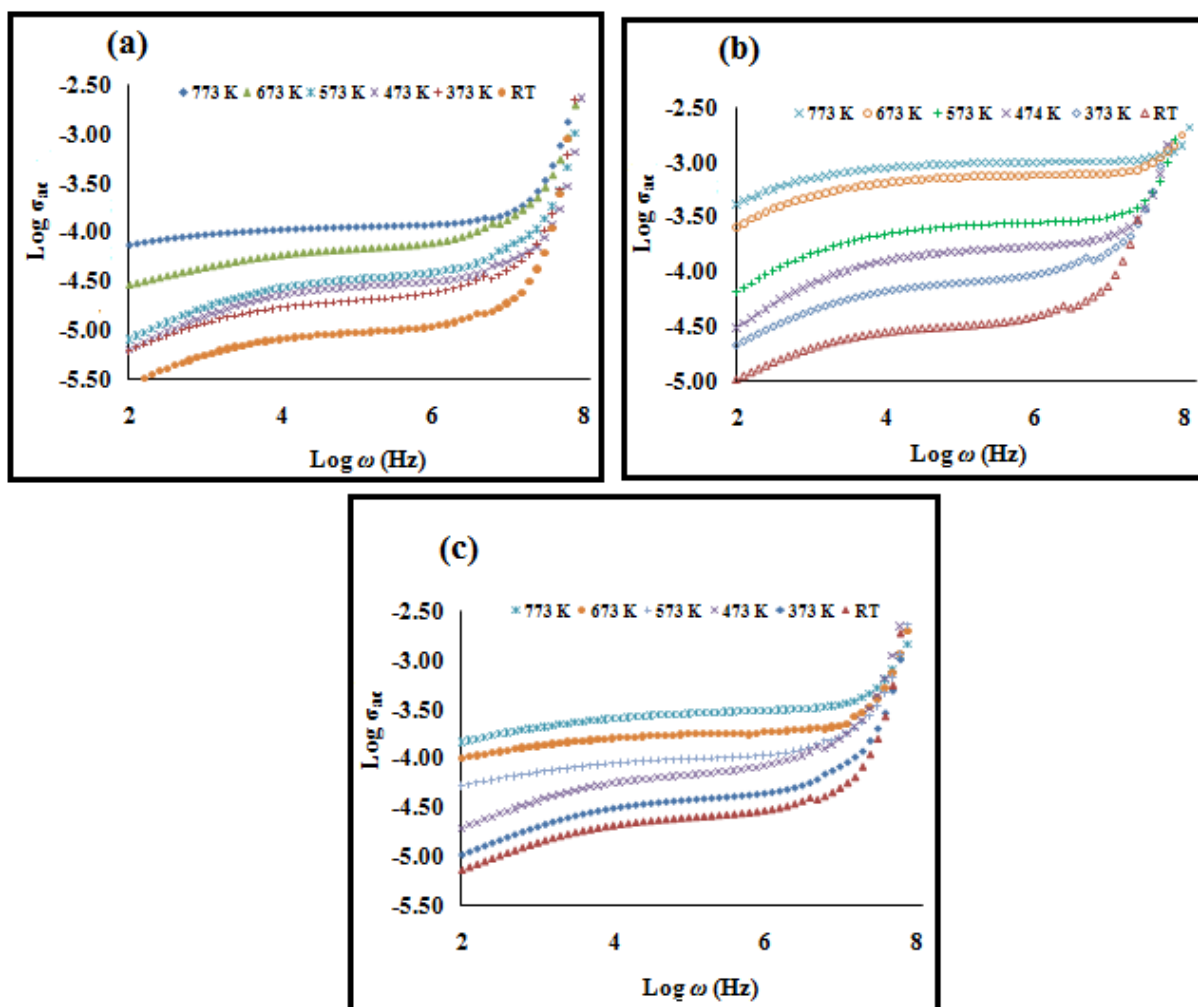


Figure 4. Conductivity spectra for (a)  $\text{Li}_4\text{SiO}_4$  (b)  $\text{Li}_{3.88}\text{Zn}_{0.06}\text{SiO}_4$  and (c)  $\text{Li}_{3.76}\text{Zn}_{0.12}\text{SiO}_4$



According to the jump relaxation model, which takes account of the coulomb interaction between mobile ions, the exponent of the power law in Eq. (6) relates to ratio of [2,34,37-38]:

$$\alpha = \frac{\text{backhop rate}}{\text{site relaxation rate}} \quad (7)$$

The backhop is the backward motion of a hopping ion to its initial site, which is caused by the coulomb repulsive interaction between mobile ions. The site relaxation is the shift of a site potential minimum to the position of the hopping ion, which is caused by a rearrangement of neighboring ions. The decrease in  $\alpha$  with zinc doping (Table 4) may be due to the formation of vacant sites for Li ion migration, which in turn reduces the backhop rate and hence decreases  $\alpha$ .

According to Almond and West [32-35,39-40], the hopping rate of ion in a material is valuable information to elucidate the ionic conduction. The ionic hopping rate,  $\omega_p$  can be obtained directly from a.c conductivity data since it corresponds to  $\sigma(\omega) = 2\sigma(0)$  [32-33, 38]. The charge carrier concentration,  $C$  can be calculated from the definition for the dc conductivity of the ion conducting material which is given by [32-35, 39-40]:

$$C = \frac{\sigma_{dc} T}{\omega_p} \quad (8)$$

where

$$C = n(1-n)N(e^2 a^2 \gamma k^{-1}) \quad (9)$$

Here  $e$  is electron charge,  $\gamma$  is correlation factor which is set equal to 1,  $N$  is equivalent site per unit volume and  $a$  is the jump distance between two adjacent sites for the ions to hop which is assumed to be 3Å for all materials [33-34].  $n$  is concentration of mobile ions which can be calculated using Eq. 9 and  $k$  is Boltzmann constant. The ionic mobility,  $\mu$  can be calculated using equation:

$$\mu = \frac{\sigma_{dc}}{ne} \quad (10)$$

The values of  $\omega_p$ ,  $C$ ,  $n$ ,  $\mu$  and  $\alpha$  for sample  $\text{Li}_{4-2x}\text{Zn}_x\text{SiO}_4$  samples at various temperatures are tabulated in Table 4. From the table, the charge carrier concentration,  $C$  and mobile ion concentration,  $n$  are constant over temperature range studied for all samples. This implies that all the lithium ions which are responsible for the conductivity are in mobile state thus can be best represented by the strong electrolyte model [32, 34-35, 40]. As such, the higher conductivity observed for  $\text{Li}_{3.88}\text{Zn}_{0.06}\text{SiO}_4$  is due to high mobile ion concentration ( $\sim 10^{26}$ ) compared with that ( $\sim 10^{25}$ ) observed for both  $\text{Li}_4\text{SiO}_4$  ( $x = 0$ ) and  $\text{Li}_{3.76}\text{Zn}_{0.12}\text{SiO}_4$  ( $x = 0.16$ ).

Meanwhile, the mobility of ions,  $\mu$  increases with increasing temperature in all samples. This means that the increase in conductivity with increasing temperature in all samples can be attributed to

the increase in ionic mobility since the density of mobile ions is constant over the temperature range studied [32-33,38]. The ion mobility value is higher in  $\text{Li}_{3.88}\text{Zn}_{0.06}\text{SiO}_4$  sample compared to  $\text{Li}_{3.76}\text{Zn}_{0.12}\text{SiO}_4$  sample. This may be attributed to the existence of ZnO impurities which distorted the crystal lattice in the sample and decreases the mobility of ions as well as the mobile ion concentration.

**Table 4.** Values of  $\omega_p$ ,  $C$ ,  $n$ ,  $\mu$  and  $\alpha$  at various temperatures for sample  $\text{Li}_{4-2x}\text{Zn}_x\text{SiO}_4$  ( $x = 0, 0.06$  and  $0.12$ )

Samples	$T$ (K)	$\omega_p$ (kHz)	$C$ ( $\text{S cm}^{-1} \text{K Hz}^{-1}$ )	$n$ ( $\text{cm}^{-3}$ )	$\mu$ ( $\text{cm}^2 \text{V}^{-1} \text{s}^{-1}$ )	$\alpha$
$x = 0$	303	818	$3.46 \times 10^{-9}$	$5.72 \times 10^{25}$	$1.02 \times 10^{-12}$	0.91
	373	2150	$3.46 \times 10^{-9}$	$5.72 \times 10^{25}$	$2.17 \times 10^{-12}$	0.85
	473	3850	$3.44 \times 10^{-9}$	$5.68 \times 10^{25}$	$3.06 \times 10^{-12}$	0.84
	573	5750	$3.44 \times 10^{-9}$	$5.68 \times 10^{25}$	$3.77 \times 10^{-12}$	0.81
	673	13520	$3.48 \times 10^{-9}$	$5.75 \times 10^{25}$	$7.57 \times 10^{-12}$	0.71
	773	22387	$3.45 \times 10^{-9}$	$5.70 \times 10^{25}$	$1.09 \times 10^{-11}$	0.62
$x = 0.06$	303	1470	$6.69 \times 10^{-9}$	$1.11 \times 10^{26}$	$1.95 \times 10^{-12}$	0.74
	373	4435	$6.67 \times 10^{-9}$	$1.10 \times 10^{26}$	$4.48 \times 10^{-12}$	0.64
	473	11519	$6.65 \times 10^{-9}$	$1.10 \times 10^{26}$	$9.15 \times 10^{-12}$	0.54
	573	22710	$6.78 \times 10^{-9}$	$1.12 \times 10^{26}$	$1.33 \times 10^{-11}$	0.45
	673	56182	$6.66 \times 10^{-9}$	$1.10 \times 10^{26}$	$3.14 \times 10^{-11}$	0.35
	773	125892	$6.63 \times 10^{-9}$	$1.10 \times 10^{26}$	$5.65 \times 10^{-11}$	0.20
$x = 0.12$	303	1950	$4.04 \times 10^{-9}$	$2.41 \times 10^{25}$	$6.69 \times 10^{-12}$	0.90
	373	3650	$4.09 \times 10^{-9}$	$2.44 \times 10^{25}$	$1.02 \times 10^{-11}$	0.84
	473	8110	$4.08 \times 10^{-9}$	$2.43 \times 10^{25}$	$1.78 \times 10^{-11}$	0.80
	573	14125	$4.06 \times 10^{-9}$	$2.42 \times 10^{25}$	$2.56 \times 10^{-11}$	0.71
	673	29900	$4.05 \times 10^{-9}$	$2.42 \times 10^{25}$	$4.62 \times 10^{-11}$	0.64
	773	57900	$4.00 \times 10^{-9}$	$2.39 \times 10^{25}$	$7.79 \times 10^{-11}$	0.51

### 3.3.3 Lithium Transference Number

Figure 5(a) presents the plot of current versus time for the  $\text{Li}/ \text{Li}_{3.88}\text{Zn}_{0.06}\text{SiO}_4/\text{Li}$  cell. The impedance plot for the cell before and after polarization is shown in Figure 5(b). The value of  $R_e$ ,  $R_{ss}$ ,  $I_{ss}$  and  $\tau_{\text{Li}^+}$  obtained from this measurement are listed in Table 5. Calculation of  $\text{Li}^+$  transference number was done using Eq. 3. The lithium transference number value is found to be 0.82. This value shows that the majority charge carrier in the sample are  $\text{Li}^+$  ions and is reasonable value for lithium battery application [41].

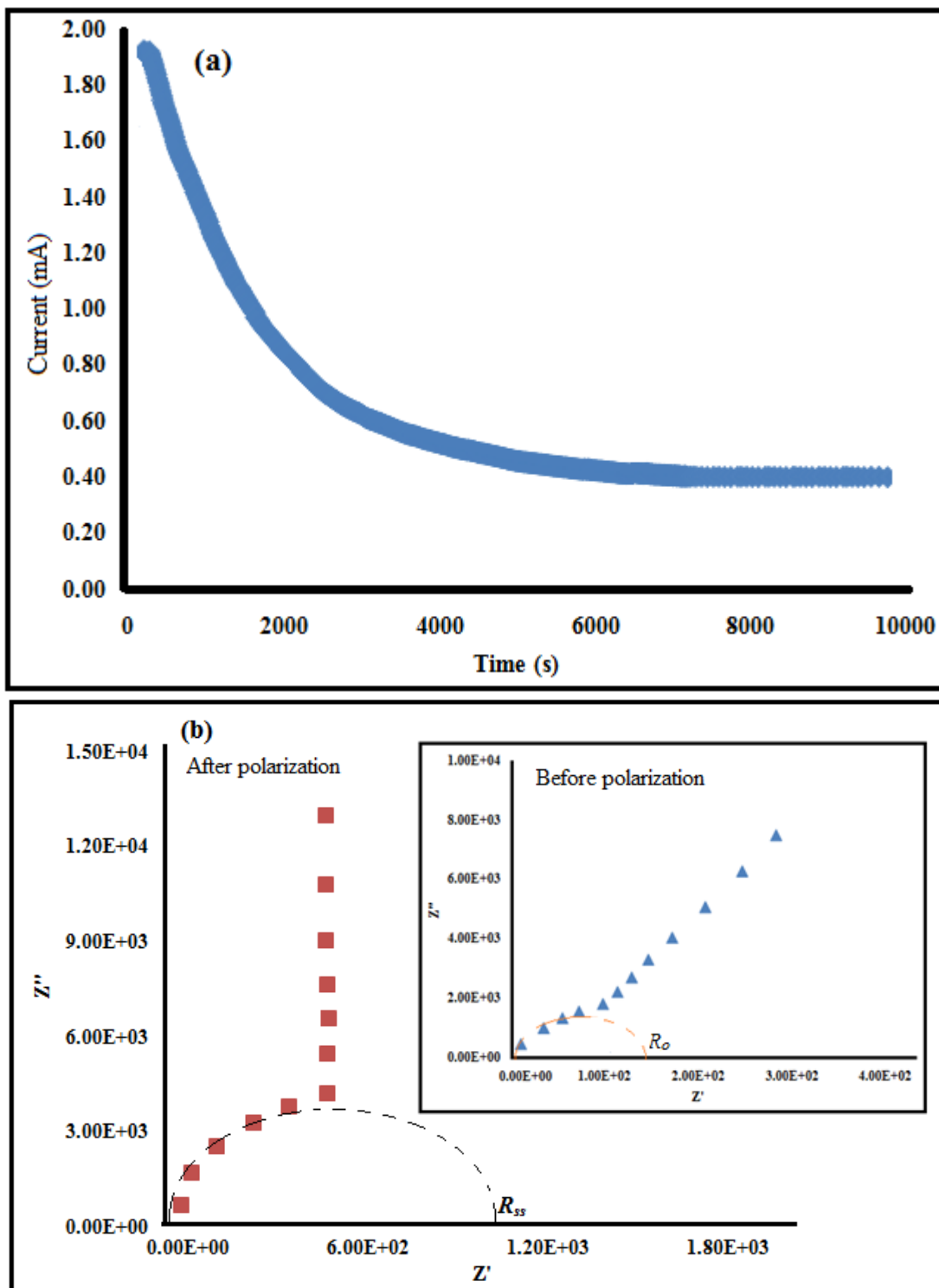


**Figure 5.** (a) Current verses time plot for  $\text{Li}_{3.88}\text{Zn}_{0.06}\text{SiO}_4$  sample and (b) Impedance response of the sample before and after dc polarization.

**Table 5.** Data obtained from lithium transference number measurement of the  $\text{Li}_{3.88}\text{Zn}_{0.06}\text{SiO}_4$  sample

Sample	$\Delta V(\text{mV})$	$I_{ss}(\text{mA})$	$R_{ss}(\Omega)$	$R_e(\Omega)$	$\tau_{\text{Li}}^+$
$\text{Li}_{3.88}\text{Zn}_{0.06}\text{SiO}_4$	500	0.384	$1.13 \times 10^3$	$1.41 \times 10^2$	0.82

#### 4. CONCLUSIONS

The effect of Zn doping on  $\text{Li}_4\text{SiO}_4$  was studied by XRD, DSC and EIS. The XRD result shows that Zn is successfully inserted into the  $\text{Li}_4\text{SiO}_4$  structure. Meanwhile the DSC result reveals that doping with Zn increases thermal stability of the compound. The RT conductivity of the Zn doped compound is an order of magnitude higher compared to the undoped  $\text{Li}_4\text{SiO}_4$ . The conductivity–temperature study shows that the entire compound obeys the Arrhenius law. The conductivity parameters such as hopping frequencies, charge carrier concentration and mobile ion concentration have been calculated by fitting the conductance spectra to power law variation. The data of these parameters prove that increase in conductivity with temperature is due to increase in ion mobility. The value of lithium transference number in the sample with  $x = 0.06$  is 0.82 and reasonable value for application in lithium batteries.

#### ACKNOWLEDGMENTS

Financial support by University of Malaya research grant (PV027/2012A) is gratefully acknowledged.

#### References

1. M. Parka, X. Zhanga, M. Chunga, G. B. Lessa, A. M. Sastrya, *J. Power Sources*, 195 (2010) 7904.
2. S.B.R.S Adnan, N.S Mohamed, *Mater. Res. Innovations*, 16 (2012) 281.
3. S.B.R.S Adnan, N.S Mohamed, K.A Norwati, *World academy of science, engineering and technologists*, 50 (2011) 670.
4. J.B Chavarria, P. Quintana, A. Huanosta, *Solid state Ionics*, 83 (2006) 24.
5. M. Wakihara, T. uchida, T. Gohara, *Solid state Ionics*, 31 (1988) 17.
6. Y. Saito, K. Ado, T. Asai, H. Kageyama, O. Nakamura, *Solid State Ionics*, 47 (1991) 149.
7. C. Masquelier, M. tabuchi, T. Takeuchi, W. Soizumi, H. Kageyama, O. Nakamura, *Solid State Ionics*, 79 (1995) 98.
8. Y. Saito, T. Asai, K. Ado, H. Kagayema, O. Nakamura, *Solid state Ionics*, 40/41 (1990) 34.
9. E.I Burmakin, *Solid State Ionics*, 36 (1988) 155.
10. A.R West, *Appl. Electrochem.*, 3 (1973) 327.
11. A. Khorassani, A. R West, *Solid State Chem.*, 53 (1984) 369.
12. A. Khorassani, A. R West, *Solid State Ionics*, 7 (1982) 1.
13. A. R Rodger, J. Kuwano, A.R West, *Solid State Ionics*, 15 (1985) 185.
14. Y. Tao, D. Yi, J. Li, *Solid State Ionics*, 179 (2008) 2396.
15. R.I Smith, A. R West, *Solid State Chem.*, 93 (1991) 436.
16. R.I Smith, A. R West, *Solid State Chem.*, 88 (1990) 564.
17. I. Hodge, M.D Ingram, A.R West, *American Ceramic Soc.*, 59 (1976) 360.
18. P.P Kumar, S. Yashonath, *Chem. Sci.*, 118 (2006) 135.
19. X. Song, M. Jia, R. Chen, *J. Mater. Processing Technol.*, 120 (2002) 21.
20. R. Adnan, N. A Razana, I. A Rahman and M. Akhyar Farrukh, *J. Chinese Chem. Soc.*, 57(2010) 222.
21. R.I Smith, A.R West, *Solid State Chem.*, 88 (1990) 564.
22. P. G. Bruce, J. Evans, C. A. Vincent, *Solid State Ionics* 28–30 (1988) 918.
23. M. Riley, S. Peter, Fedkiw, S. A. Khan, *Electrochem. Soc.*, 149 (2002) A667.
24. A.M.M. Ali, M.Z.A Yahya, H. Nahron, R. H. Y. Subban, *Ionics*, 12 (2006) 303.
25. D. Tranqui, R.D Shannon, H.Y Chen, *Acta Crystallogr.*, 35 (1979) 2479.

26. B.L Dubey, A.R West, *J. Inorg. Nuclear Chem.*, 35 (1973) 3713.
27. S. Zhang, C. Deng, B.L Fu, S.Y Yang, L. Ma, *Electrochim. Acta*, 55 (2010) 8482.
28. H. Kleykamp, *Thermochim. Acta*, 287 (1996) 191.
29. G.W Hollenberg, *J. Nuclear Mater.*, 103 (1981) 591.
30. D. Vollath, H. Wedemeyer, H. Zimmermann, H. Werle, *J. Nuclear Mater.*, 174 (1990) 86.
31. M. Dudek, *Int. J. Electrochem. Sci.*, 7 (2012) 2874.
32. S.B.R.S Adnan, N.S. Mohamed, *Int. J. Electrochem. Sci.*, 7 (2012) 9844.
33. L. P. Teo & M. H. Buraidah & A. F. M. Nor & S. R. Majid, *Ionics* 18 (2012) 655.
34. M. Vijayakumar, G. Hirankumar, M.S. Bhuvaneshwari, S. Selvasekarapandian, *J. Power Sources*, 117 (2003) 143.
35. T. Savitha, G. Hirankumar, M.S. Bhuvaneshwari, S. Selvasekarapandian, C.S. Ramya, R. Baskaran, P.C Angelo, *J. Power Sources*, 157 (2006) 553.
36. A.M. Abo El Ata, S.M. Attia, T.M Meaz, *Solid State Sci.*, 6 (2004) 61.
37. K. Funke, *Solid State Ionics*, 94 (1997) 27.
38. M.A Afifi, M.EL-Nahass, A.E Bekheet, I.T Zedan, S.R Elliot, *Physica B : Physics of Condensed Matter*, 400 (2007) 248.
39. D.P Almond, A.R West, *Solid State Ionics*, 9&10 (1983) 277.
40. D.P Almond, A.R West, *Solid State Ionics*, 23 (1987) 27.
41. Yongxin An, Pengjian Zuo, Xinqun Cheng, Lixia Liao, Geping Yin, *Int. J. Electrochem. Sci.*, 6 (2011) 2398 .